

Gaussian Mode Analysis of THz Horn using CST Microwave Studio

Monika Sharma², Surbhi Adya^{2,*}, Rajendra Kumar Verma^{1,2}, Shivendra Maurya^{1,2}, V.V.P Singh²

¹Academy of Scientific and Innovation Research (AcSIR),

²Council of Scientific and Industrial Research - Central Electronics Engineering Research Institute (CSIR-CEERI),
Pilani, Rajasthan 333031, India.

*surbhiadya@gmail.com

Abstract- This paper presents the theoretical investigation done in analysis of the Gaussian modes of the rectangular pyramidal horn at 0.17THz or 170GHz by using CST Microwave Studio to assess their generated modes. The results revealed the generation of combination of TEM_{0,0} and TEM_{2,0} mode. Using the resultant generated TEM mode, an alumina RF window at 170GHz was characterized via free space test setup. On the basis of above analysis it is concluded that horn antenna has harmonics as its dominant mode and not the fundamental mode. It produces a non-gaussian mode.

Index Terms—High power microwaves, Gaussian beam propagation, CST Microwave Studio, MATLAB, Pyramidal horn antenna, TEM modes, Alumina RF Window.

I. INTRODUCTION

A pyramidal horn antenna is a four-sided shaped pyramid, with a rectangular [6] cross section (Fig. 1). They are a common type, used with rectangular waveguides, and radiate linearly polarized radio waves. It is the simplest and the best horn as it has equal radiation patterns in both E-plane and H-plane along with its high gain and directivity. These antennas are widely used in various applications in the microwave range due to its robustness, high gain, moderate bandwidth, simple construction, easy excitation and low voltage standing wave ratio VSWR and are very popular at UHF and higher frequencies. Horn antennas have a wide impedance-bandwidth, implying that the input impedance is fairly constant over a wide frequency range. The design parameters for window and antenna are listed in Table I and II. They are sufficiently good match for most applications, and they are far easier and much cheaper to fabricate. There are several computer tools available to characterize them.

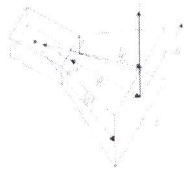


Figure 1. Geometry of a pyramidal horn.

TABLE I
PARAMETERS FOR ALUMINA WINDOW ELECTROMAGNETIC SIMULATIONS

Parameter	Value
Material	99.5% Alumina($\epsilon_r=9.5$)
Disc diameter, D_1	90mm
Disc thickness, t	3mm
Window aperture/waveguide diameter, D	80mm
Circular waveguide length, L	15mm
Waveguide Wall thickness, t_w	4mm

TABLE II
PARAMETERS FOR HORN ANTENNA DESIGN

Parameter	Value
Horn cross-section dimension	A=14mm B=10.9mm
Horn length	26.4 mm
Horn beam width	6.6°
Horn feed mode	TE ₁₀
Horn far field mode	TEM

The design, simulation and characterization of the antenna and window have been done on CST Microwave Studio in order to verify the simulated and the practical (experimental setup) results. Hence, the pyramidal horn and the window are characterized.

II. DESIGN

It is a half-wave resonant window Transmission Line Theory which predicts that the window will be resonant at all those frequencies for which the alumina disc [4] thickness follows the following relation.

$$t = n\lambda_g/2$$

The expression for the electric field is given by the below equation [5].

$$E(r, z) = \left(\frac{2}{\pi W^2} \right)^{0.5} \exp \left(\frac{-r^2}{W^2} - jkz - \frac{j\pi r^2}{\lambda R} + j\phi_0 \right)$$

The alumina window and pyramidal horn antenna [8, 9] with the given design parameters has been modelled in Computer Simulation Tool Microwave Studio(CST-MWS) software for their characterization (Fig. 2 and Fig. 3).

In order to determine the S-parameters of designed window in CST-MWS, a free space experimental test setup [11] has been used as shown in Fig.4. The major instruments of the experimental set-up [12] are PNA E8364C which is a commercial product of Agilent Technologies, with VNA extender modules which provide 140-220 GHz frequency span. A waveguide calibration kit containing open, short, load, is also provided for calibration of the test set-up. Two pyramidal horn antennas are used for the measurement. In this one end of the VNA via PNA is connected to the transmitting horn antenna and other end with the receiving horn antenna. In between the two horns window is kept for its testing and characterization and the results (S-parameters) are displayed on the VNA screen.

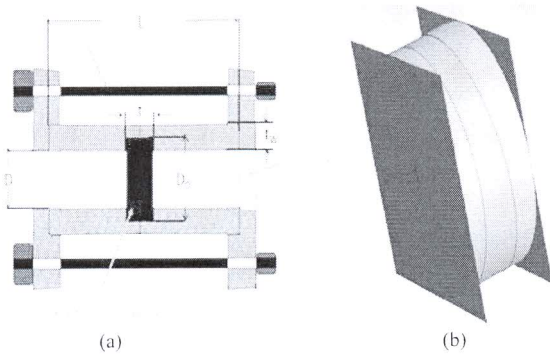


Figure 2.(a) Schematic geometry (b) CST-MWS simulated model of Alumina Window.

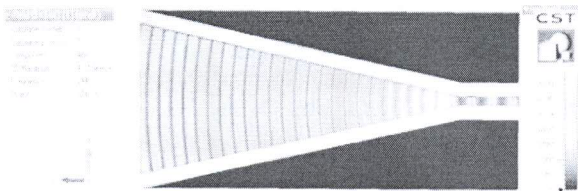


Figure 3.CST-MWS simulated model of Pyramidal Horn Antenna.

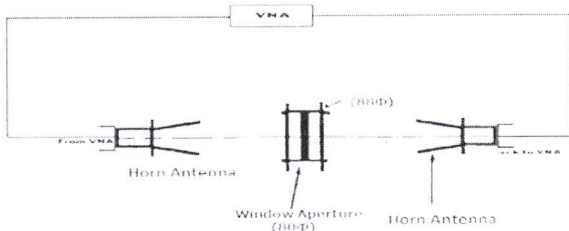


Figure 4.Free space test setup for alumina window characterization.

The CST-MWS simulated results, S-parameters (S_{11} in dB), of the designed window with its resonant pattern for TE_{11} mode between 140 and 220 GHz is shown in Fig. 5. The CST-MWS simulated pyramidal horn antenna modes as given in the Fig.6 depicts (a) the top view and side view of the $TEM_{0,0}$ modes (b) the top view and side view of the $TEM_{2,0}$ modes (c) the $TEM_{2,0}$ mode takes over the $TEM_{0,0}$ mode.

Hence, it is concluded that the horn does not produce a pure fundamental mode and has a combination of both the modes. Conclusively, it is a non-gaussian mode.

The S-parameters and VSWR of the CST-MWS simulated model of the pyramidal horn are shown in Fig. 7. Also, its polar plot and 3D plot of radiation pattern is shown in Fig.8.

The main lobe is 26.2dBi and the side lobe is -8.7dB. The number of side lobes is more and therefore, which is decreasing the power in the main lobe [10].

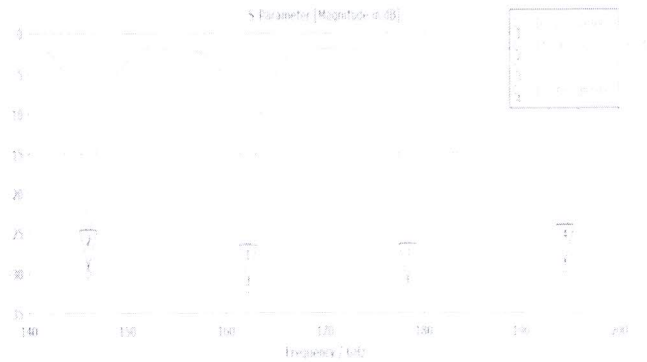


Figure 5.CST-MWS simulated frequency response of window with TE_{11} mode.

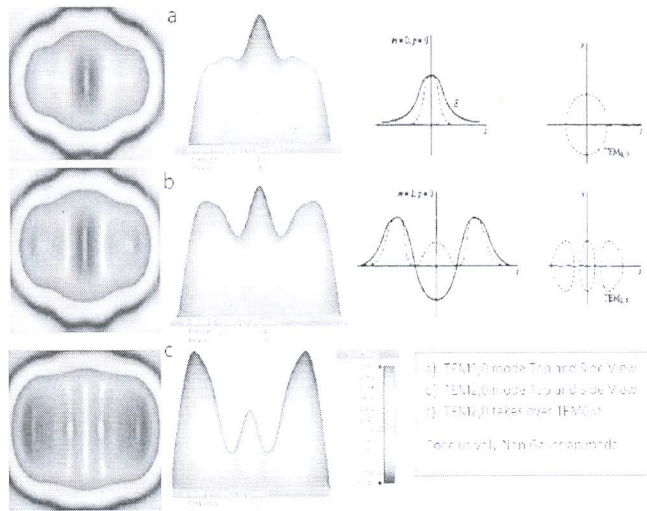


Figure 6.CST-MWS simulated pyramidal horn antenna modes.

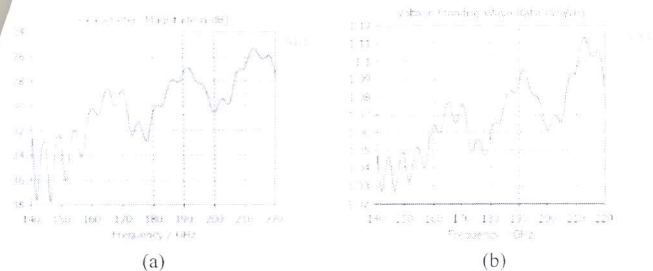


Figure 7. (a) S-Parameters and (b) VSWR of CST-MWS simulated model of pyramidal horn antenna.

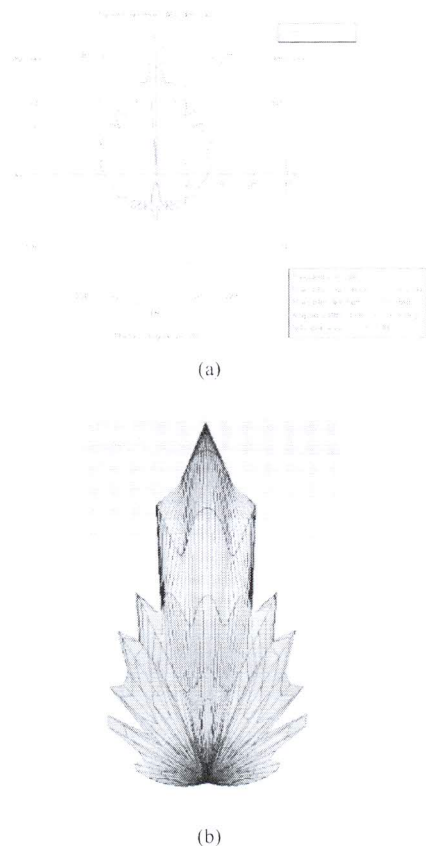
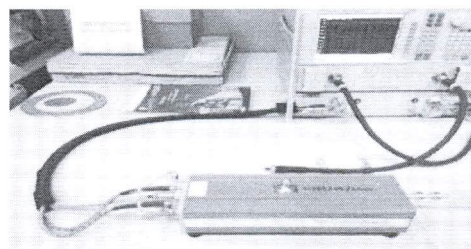


Figure 8. (a) Polar plot and (b) 3D plot radiation pattern of the CST-MWS simulated model of pyramidal horn antenna.

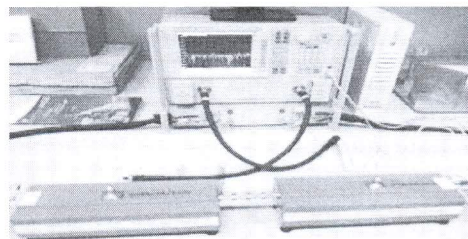
V.RESULTS &DISCUSSIONS

Firstly, the test set up was calibrated in the frequency range 140-220 GHz. Two port calibrations were performed using open, short (Fig.9a) and through (Fig.9b) kits provided with PNA. The test window assembly was then inserted midway between the horns as shown in Fig. 11(a) and the measurements were carried out [12] [13] [14].

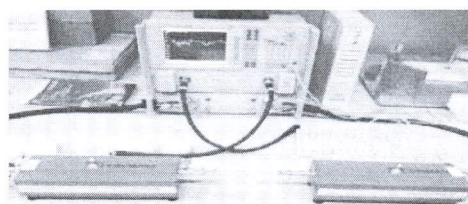
The horn feed (input) is WR5 (TE_{10} mode). Its outer cross section and length are $A_{14mm} \times B_{10.9mm}$ and 26.4 mm respectively. The horn has beam-width of 6.6° through which we can decide



(a)



(b)



(c)

Figure 9. Calibration of experimental set up (a) Open & Short (b) Through (c) referencing using pyramidal horns.

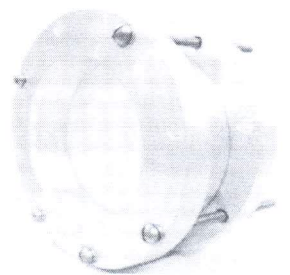


Figure 10. Fabricated window with assembly.

the location of measuring device according to its required diameter. Near field mode for horn antenna is same as feed, i.e., TE_{10} with lower amplitude and far field mode is TEM mode.

The horns are attached at the output of VNA extender modules and aligned at a gap distance of 14.5cm to set the reference for S_{11} measurements.

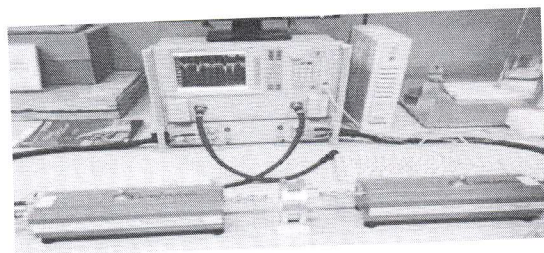
The practical results (Fig.11b) of the experimental test setup and the simulated results of the window are obtained and have similar resonant peaks as shown in TABLE IV.

TABLE III
PARAMETERS FOR EXPERIMENTAL SETUP

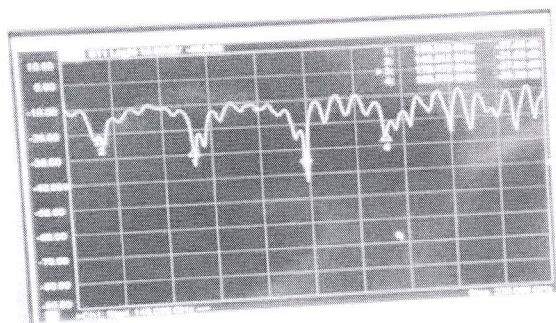
Parameter	Value
Frequency	140-220GHz
Distance between horns	14.5cm
Window position	(Mid-plane (5.5cm))
Mode	TEM

TABLE IV
MEASURED VS SIMULATED RESULTS

Resonant Frequencies	Measured (TEM)	Simulated (TE ₁₁)
f ₁	145.6	145.06
f ₂	160.8	161.2
f ₃	179.4	178.3
f ₄	193.01	193.4



(a)



(b)

Figure 11. (a) S₁₁(dB) measurements of the window assembly (b) Practical S₁₁(dB) results.

VI. CONCLUSION

The alumina window is characterized using two pyramidal horn antennas shown in the experimental test setup in Fig.8 (a). The CST-MWS simulated results of the window in Figure.5 and the practical results obtained from the test setup in Fig.8(b) depicts that both have the similar nature of the resonant peaks as shown in TABLE IV.

It can be concluded from the CST-MWS simulated model of the pyramidal horn antenna used in the experimental setup, that it does not produce the pure fundamental mode but generates a combination of TEM_{0,0} and TEM_{2,0} modes. It produces a non-gaussian mode.

Therefore, in the future, further improvement of this free space experiment can be done by using a corrugated or a conical horn antenna instead of the pyramidal horn antenna in the experimental test setup for window characterization in order to enhance the results.

ACKNOWLEDGMENT

Authors are thankful to the Director, CSIR-CEERI, Pilani for his kind permission to publish this work. This work has been carried out as a part of the CSIR network project. Authors are also thankful to other team members for their co-operation and time to time valuable suggestions for the improvement of the work.

REFERENCES

- [1] Adrain Dobroiu, Chikootani, Kodo Karwase, "Terahertz-wave Sources and imaging applications", IOP Meas. Technol. 17, R161-R174, 2006.
- [2] ITER-the way to new energy, <https://www.iter.org/project>
- [3] Manfred Thumm, "High Power Gyro-Devices for Plasma Heating and Other Applications", International Journal of Infrared and Millimeter Waves, vol.26, no.4, April, 2005.
- [4] G. Taylor, M.E. Austin et al, "Status of the design of the ITER ECE diagnostic", Princeton Plasma Physics Laboratory Report, PPPL-5026, November, 2014. (http://bp.pppl.gov/pub_report/2014/PPPL-5026.pdf)
- [5] Paul F. Glodsmith, "Quasi-Optical Systems", IEEE press 445 hoes lane, ch.1-2, 1998.
- [6] F. A. Benson, "Attenuation of rectangular waveguides, in millimeter and sub-millimeter waves", Iliffe Press, London, ch.14, 1969.
- [7] Paul F. Goldsmith, "Quasi-optical techniques", IEEE Invited Paper in Proceedings of the IEEE, vol. 80, no. 11, pp. 1729-1747, November, 1992.
- [8] H. Kogelnik and T. Li "Laser beam and resonators", Proceedings of the IEEE, vol.54, no.10, pp.1312-1329, October, 1966.
- [9] M. Thumm, "Passive high power microwave components", IEEE Trans Plasma Science, vol. 30, issue 3, pp755-786, June 2002.
- [10] Corrado Dragone, "Attenuation and radiation characteristics of the HE₁₁-mode", IEEE Transactions on Microwave Theory and Techniques, vol. MTT-28, no. 7, pp. 704-710, July, 1980.
- [11] B. Maffei, S. Legg, M. Robinson et al, "Implementation of a Quasi-Optical Free-space S-Parameters Measurement System", 35th ESA Antenna workshop on Antenna and Free-space RF Measurement, The Netherlands, 10-13 September, 2013.
- [12] Richard Collier, Doug Skinner, "Microwave Measurements", 3rd edition 2007, IET, London, UK.
- [13] Philip G. Bartley, Jr. and Shelley B. Begley, "Improved free-space S-parameter calibration", IMTC 2005-Instrumentation and Measurement Technology Conference Ottawa, pp. 372-374, Canada, 17-19 May, 2005.
- [14] D. K. Ghodgaonkar, V. V. Vardhan, and V. K. Vardhan, "A free space method for measurements of dielectric constants and loss tangents at microwave frequencies", IEEE Trans. of Instrum. Meas., vol. 38, no 3, pp. 89-793, June 1989.